Discussion on the mode mixing in wave energy control systems using the Hilbert-Huang transform

Paula B. Garcia-Rosa, Marta Molinas, and Olav B. Fosso

Abstract—**A great improvement in the absorption of energy of a wave energy converter (WEC) is obtained with a time-varying power take-off (PTO) damping over a constant damping. In a passive control scheme based on the Hilbert-Huang transform (HHT), the PTO damping is time-varying and tuned to the instantaneous frequency of the wave excitation force. The HHT method relies on the use of the empirical mode decomposition (EMD) method to decompose the wave signal into a number of components (IMFs) from the highest to the lowest frequency component. However, the decomposition process is not always perfect and may result in mode mixing, where an IMF will consist of signals of widely disparate frequency scales, or different IMFs will consist of signals with similar frequency scales. Mode mixing can be caused by intermittent/noisy signals, and by specific amplitude and frequency relations of the original modes in the signal. The aim of this paper is to extend the studies on the use of the HHT for WEC tuning purposes by revealing how the EMD mode mixing problem affects the WEC performance. A comprehensive study using firstly synthetic two-tone waves (i.e., superposition of two sinusoidal waves) is performed. Then, the observations from the two-tone studies are used to further improve the energy absorbed by WECs using the HHT in real ocean wave scenarios resembling the analytic scenario.**

Index Terms—**wave energy, Hilbert-Huang transform, mode mixing.**

I. Introduction

RECENT studies have shown that tuning the power take-off (PTO) damping of a wave energy converter (WEC) to time-frequency estimations obtained from the Hilbert-Huang transform (HHT) results in greater energy absorption than tuning the PTO to a constant frequency of the wave spectrum [1], or to time-frequency estimations from the extended Kalman filter (EKF), and frequency-locked loop (FLL) method [2]. Both the EKF and FLL methods provide single dominant frequency estimates, whereas the HHT provides the instantaneous wave-to-wave frequency of the oscillation modes present in a wave profile. In addition, by adopting other methods to, e.g., estimate the online dominant wave frequency [3], or determine the optimal time-varying PTO damping [4], other studies have also shown that continuously tuning the PTO result in greater energy absorption than tuning it to a constant frequency of the wave spectrum.

The HHT method [5] relies on the use of the empirical mode decomposition (EMD) to decompose the wave signal into a number of components, named intrinsic mode functions (IMFs), from the highest to the lowest frequency component. However, the decomposition process may result in mode mixing, and an IMF will consist of signals of widely disparate frequency scales, or different IMFs will consist of signals with similar frequency scales [6]. Mode mixing can be caused by an intermittent/noisy signal, by specific amplitude and frequency relations of the original modes in the signal, and by a combination of both cases. Additionally, the mode mixing effects can be attenuated by applying, e.g., masking signals prior to the EMD procedure [7] [8], or by using the ensemble EMD (EEMD), a white noise-assisted EMD method [9].

Focusing on the case when mode mixing is caused by specific amplitude and frequency relations of the original modes in a signal, [10] presents a rigorous mathematical analysis that shows how the EMD separates the original modes in signals with two frequency components. Three different domains are identified by the authors depending on the frequency and amplitude ratios of the modes. After the EMD procedure, the components can be separated and correctly identified (domain 1), considered as a single wave-form (domain 2), or the EMD does something else (domain 3) [10].

In this paper, the focus is also on mode mixing caused by specific amplitude/frequency relations of original modes in a wave signal. In this framework, the aim is to extend the studies on the use of the HHT for WEC tuning purposes with a passive control (PC) strategy, by revealing how the EMD mode mixing problem affects the WEC performance. A comprehensive study using initially synthetic two-tone waves (superposition of two sinusoidal waves) is performed. Then, the mode mixing conditions observed for the two-tone wave studies are used to further improve the energy absorbed by WECs using the HHT in real ocean wave scenarios resembling the synthetic two-tone wave scenario.

II. Passive Control using the HHT

Here, we assume linear hydrodynamic theory, and consider a single oscillating-body represented as a truncated vertical cylinder constrained to move in heave. By neglecting friction and viscous forces, the

ID 1275 track GPC.

P. B. Garcia-Rosa and O. B. Fosso are with the Department of Electric Power Engineering, Norwegian University of Science Technology, Trondheim, Norway (e-mails: p.b.garcia-rosa@ieee.org, olav.fosso@ntnu.no).

M. Molinas is with the Department of Engineering Cybernetics, Norwegian University of Science Technology, Trondheim, Norway (e-mail: marta.molinas@ntnu.no).

heave motion $x(t)$ of the floating cylinder is described by:

$$M\ddot{x}(t)+\int_0^t h_r(t\quad\tau)\,\dot{x}(\tau)\,d\tau+Sx(t)=f_e(t)+f_p(t)\,, \quad (1)$$

with the kernel of convolution term given by [11]

$$h_r(t)=\frac{2}{\pi}\int_0^{\infty} B_r(\omega)\cos(\omega t\quad\tau)\,d\omega\,, \quad (2)$$

where $M=[m+m_r(\infty)]$, m is the body mass, $m_r(\infty)$ is the infinite-frequency added mass coefficient, S is the buoyancy stiffness, $B_r(\omega)$ is the radiation damping coefficient, ω, is the wave frequency, $f_e(t)$ is the wave excitation force, and f_p is the force of the PTO mechanism.

The excitation force is calculated as

$$f_e(t)=\int_{-\infty}^{\infty} h_e(t\quad\tau)\,\zeta(\tau)\,d\tau\,, \quad (3)$$

where ζ is the wave elevation, and h_e is the inverse Fourier transform of the excitation force transfer function $H_e(\omega)$,

$$h_e(t)=\frac{1}{2\pi}\int_{-\infty}^{\infty} H_e(\omega)e^{i\omega t}\,d\omega\,, \quad (4)$$

which has low-pass filter characteristics for floating WECs. Equation (3) is non-causal, since in fact, the pressure distribution is the cause of the excitation force and not the incident waves [12].

For the passive control, the PTO force is parameterized as a function of the damping B_p,

$$f_p(t)=\quad B_p(t)\dot{x}(t)\,, \quad (5)$$

where $B_p\,2\,\mathbb{R}_+$ is continuously modified, and tuned to the excitation force frequency. Here, the PTO damping is calculated as

$$B_p(t)=\sqrt{(B_r(\hat{\omega}_d))^2+(\hat{\omega}_d(m+m_r(\hat{\omega}_d))\quad S/\hat{\omega}_d)^2}\,, \quad (6)$$

where $\hat{\omega}_d(t)$ is the instantaneous frequency of the dominant IMF component of the excitation force [1].

Prior to calculating the instantaneous frequency, the excitation force is decomposed into a number of IMF components by applying the EMD. Therefore, the dominant IMF is identified through the comparison of the energy of each IMF signal (E_{c_i}) with the energy of the excitation force signal (E_{f_e}) [1],

$$E_{c_i}=\int_0^T |c_i(t)|^2 dt\,, \quad E_{f_e}=\int_0^T |f_e(t)|^2 dt\,, \quad (7)$$

where $c_i(t)$ is the i-th IMF component. The dominant component $c_d(t)$ is the IMF with the highest E_{c_i}/E_{f_e} ratio. The Hilbert transform (HT) is then applied to $c_d(t)$ [5]:

$$v_d(t)=\frac{1}{\pi}\,P\int_{-\infty}^{\infty}\frac{c_d(\tau)}{t\quad\tau}d\tau\,, \quad (8)$$

where P indicates the Cauchy principal value. Thus, the dominant IMF is represented as an analytic signal,

$$z_d(t)=c_d(t)+jv_d(t)\,, \quad (9)$$

with amplitude $\hat{A}_d$, phase $\hat{\phi}_d$, and instantaneous frequency $\hat{\omega}_d$, respectively estimated as

$$\hat{A}_d(t) = \sqrt{c_d^2(t)+v_d^2(t)}\,, \quad (10)$$

$$\hat{\phi}_d(t) = \arctan\left(\frac{v_d(t)}{c_d(t)}\right)\,, \quad (11)$$

$$\hat{\omega}_d(t) = \dot{\phi}_d(t)\,. \quad (12)$$

Furthermore, the extracted energy by the WEC over a time range T is calculated as

$$E_a(t)=\quad\int_0^T \dot{x}(t)f_p(t)\,dt\,, \quad (13)$$

where $\dot{x}$ is the body velocity.

III. EMD AND MODE MIXING

The calculation of the instantaneous frequency by applying the HT (8) directly to the excitation force signal results in negative local frequencies, as the instantaneous frequency is not well defined for multicomponent signals [13], i.e. signals with more than one local extrema for each zero crossing. Thus, $f_e(t)$ is decomposed into monocomponent signals (IMFs) using the EMD. An intrinsic mode function is a signal that is symmetric with respect to the local zero mean, and has numbers of zero crossings and extrema differing at most by one. Therefore, an IMF satisfies the necessary conditions for a meaningful interpretation of the instantaneous frequency obtained from the HT [5].

The EMD algorithm identifies local maxima and minima of $f_e(t)$, and calculates upper and lower envelopes for such extrema using cubic splines. The mean values of the envelopes are used to decompose the original signal into IMFs, in a sequence from the highest frequency component to the lowest frequency component. The EMD algorithm is summarized in Table I. The steps 1 to 5 are known as sifting process.

TABLE I
EMD ALGORITHM.

Step 0: Set i = 1; $r(t) = f_e(t)$;
Step 1: Identify the local maxima and minima in $r(t)$;
Step 2: Calculate the upper envelope defined by the maxima, and the lower envelope defined by the minima;
Step 3: Calculate the mean envelope $m(t)$;
Step 4: Set $h(t) = r(t) - m(t)$;
Step 5: If $h(t)$ is an IMF, go to next step. Otherwise, set $r(t) = h(t)$ and go back to step 1;
Step 6: Set $c_i(t) = h(t)$; $r(t) = r(t) - c_i(t)$;
Step 7: If $i = N$, define the IMF components as $c_1(t), \ldots, c_N(t)$, and the residue as $r(t)$. Otherwise, set $i = i + 1$ and go back to step 1.

The decomposition process may result in mode mixing, and an IMF will consist of signals of widely disparate frequency scales, or different IMFs will consist of signals with similar frequency scales. Mode

mixing can be caused by an intermittent/noisy signal, by specific amplitude and frequency relations of the original modes in the signal, or by a combination of both cases. The second case is considered in this study.

In this framework, [10] presents a mathematical analysis that shows how EMD separates the original modes in signals with two frequency components. Figure 1 illustrates a summary of how EMD behaves for two-tone signals. Here, a two-tone signal represents the normalized excitation force for two wave components,

$$\bar{f}_e(t) = a\cos(\omega_1 t + \varphi) + \cos\omega_2 t\,, \tag{14}$$

$$a = a_1 j H_e(\omega_1) j (a_2 j H_e(\omega_2) j)^{\ 1}\,, \tag{15}$$

where ω_1 is the low-frequency (LF) component, ω_2 is the high-frequency (HF) component, $\varphi = \varphi_1 \quad \varphi_2$, $\varphi_1 = \angle H_e(\omega_1)$, $\varphi_2 = \angle H_e(\omega_2)$, and a_1, a_2, and φ_1, φ_2 are, respectively, the amplitudes and phases of LF and HF components. Following [10], the frequencies $f\omega_1, \omega_2 g$ and phases $f\varphi_1, \varphi_2 g$ are much lower than the sampling frequency and then, the EMD behaviour is only sensitive to the relative parameters ω_1/ω_2 and φ.

If the two components are correctly separated by the EMD, then the first IMF ($c_1(t)$) matches the high-frequency component of the signal ($\cos\omega_2 t$). Two well-defined regions (Fig. 1.a) are observed depending on the amplitude and frequency ratios of original modes: the white region indicates a perfect separation of the components ($p_1 \quad 0$), and the darkest region indicates the separation is not perfect ($p_1 \quad 1$). In such a case, the EMD either consider the signal as a single modulated component or it does something else. The separation of the components is not possible if either the frequency ratio is above the cutoff frequency $\omega_c = 0.67$ (dotted line) or the frequency and amplitude ratios are in the area above $a\left(\frac{\omega_1}{\omega_2}\right)^2 = 1$ (dashed line) [10].

In addition, it is important to distinguish between the single modulated component area and the area which EMD does something else. Notice that if the signal is a single modulated component, then the first IMF should be the original signal ($\bar{f}_e(t)$). Figure 1.b illustrates a comparison of the first IMF with the original signal for the areas $\frac{\omega_1}{\omega_2} \quad \omega_c$ and $a\left(\frac{\omega_1}{\omega_2}\right)^2 \quad 1$ (cases when the separation of components is not perfect).

Therefore, three domains are defined [10]: (D1) the components are separated and correctly identified (p_1 0); (D2) the components are considered as a single waveform ($p_2 \quad 0$); (D3) the EMD does something else (the darkest areas in Fig. 1.b, i.e., $p_2 \quad 1$). In domain D3, the components are either halfway between domains D1 and D2 or contain fake oscillations, i.e., oscillations derived from the decomposition process and not from the original modes.

IV. EMD MODE MIXING EFFECT ON THE ENERGY ABSORBED BY WECS

In this section, we investigate the effect of EMD mode mixing on the energy absorbed by WECs using the HHT for tuning purposes in a passive control strategy. The analysis will initially focus on synthetic two-tone waves and the domains to which the mode mixing belongs (D2 and D3), and then it is extended to real ocean waves that exhibit similar properties as the synthetic two-tone waves. The floating body is a heaving cylinder with mass $m = 3.2 \quad 10^5$ kg, radius of 5 meters, draught of 4 meters, and resonance frequency 1.2 rad/s [1].

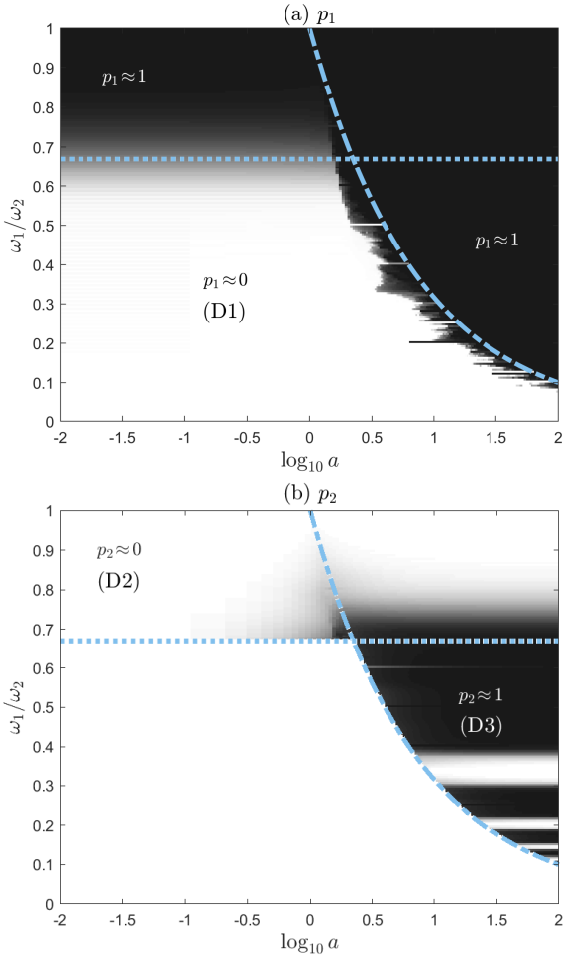

Fig. 1. EMD behavior for two tones signal (a) performance measure of separation: $p_1 = \frac{||c_1(t) - \cos\omega_2 t||}{||a\cos\omega_1 t||}$, (b) distance measure of the first IMF to the original signal: $p_2 = \frac{||c_1(t) - f_e(t)||}{||\cos\omega_2 t||}$. Dotted line: $\omega_c = 0.67$, dashed line: $a\left(\frac{\omega_1}{\omega_2}\right)^2 = 1$. (The plots are reproduced from [10] with 10 sifting iterations and sampling period of 1 ms).

A. Two-tone waves

By using two-tone waves in domains D2, and D3, as incident waves, Figures 2, and 3, compare the energy absorbed by the WEC over $T = 10$ min for the cases when HHT is used for tuning purposes (E_a) with the cases when a constant dominant frequency is used ($E_{a,D}$). The constant dominant frequency is either ω_1 or ω_2 depending on which component has the highest excitation force amplitude. Only domains D2 and D3 are considered, as in domain D1 the components are well separated and identified by the EMD. Four different frequencies are considered for the HF components: 0.75, 0.9, 1.2, and 1.5 rad/s.

The effect of the EMD mode mixing on the energy absorbed depends on both the domain (D2 or D3) and the frequency of the components, which is related to the frequency response of the floating body.

For D2 and the cases in which HF components are below the resonance frequency of the body (1.2 rad/s), the dominant IMFs are single modulated components resulting in greater absorption of energy than tuning to the constant dominant frequency (Fig. 2, top). The benefit of using the IMF modulated components is higher for the cases when the amplitudes of the excitation force are close to each other (regions around $\log_{10} a \quad 0$). However, when the resonance frequency is the HF or the LF component (Fig. 2, bottom), the single modulated IMFs can either have a positive or negative effect on the energy absorbed by the WEC. Figure 4 shows the IMF instantaneous frequency, and the PTO damping, for the case when $\omega_2 = 1.2\,\text{rad/s}$ and $E_a/E_{a,D} = 0.94$. It can be observed that the IMF frequency varies from 1.1 rad/s to 1.7 rad/s, but since the constant dominant frequency is the resonance frequency of the WEC, the energy absorption with HHT is less than with the constant frequency. Conversely, when the dominant frequency is $0.96\,\text{rad/s}$ ($\omega_1 = 0.8\omega_2$ and $a_1 jH_e(\omega_1)j > a_2 jH_e(\omega_2)j$), the HHT is superior. Table II summarizes the results for domain D2.

TABLE II
SUMMARY OF RESULTS FOR DOMAIN D2 ($\omega_1/\omega_2 = 0.8$). COMPONENTS ARE DECOMPOSED AS SINGLE WAVE-FORMS.

HF (rad/s)	Region	Dominant component	Comparison of E_a with $E_{a,D}$
0.75	$\log_{10} a < 0$	HF ($\omega_2 = 0.75\,\text{rad/s}$)	$E_a > E_{a,D}$
	$\log_{10} a > 0$	LF ($\omega_1 = 0.6\,\text{rad/s}$)	$E_a > E_{a,D}$
0.9	$\log_{10} a < 0$	HF ($\omega_2 = 0.9\,\text{rad/s}$)	$E_a > E_{a,D}$
	$\log_{10} a > 0$	LF ($\omega_1 = 0.72\,\text{rad/s}$)	$E_a > E_{a,D}$
1.2	$\log_{10} a < 0$	HF ($\omega_2 = 1.2\,\text{rad/s}$)	$E_a < E_{a,D}$
	$\log_{10} a > 0$	LF ($\omega_1 = 0.96\,\text{rad/s}$)	$E_a > E_{a,D}$
1.5	$\log_{10} a < 0$	HF ($\omega_2 = 1.5\,\text{rad/s}$)	$E_a > E_{a,D}$
	$\log_{10} a > 0$	LF ($\omega_1 = 1.2\,\text{rad/s}$)	$E_a < E_{a,D}$

Notice that the damping tuning equation (6) is not optimal for instantaneous frequency tuning. Such an equation represents the optimal damping equation for regular waves [12], i.e., sinusoidal waves with a constant frequency component. Further studies are needed to determine the best damping tuning equation when the instantaneous frequency is used as an input. As an example, if the PTO damping oscillations below $2 \quad 10^5\,\text{kg/s}$ are filtered out from the damping profile in Figure 4, the energy absorbed increases 3% when compared to the original damping obtained directly from the HHT approach and (6).

For domain D3 (Fig. 3), only the region $\log_{10} a > 0$ is considered, as indicated by Fig. 1.b. Therefore, the LF component (ω_1) is the dominant component for all the cases, and the HHT is superior in all such cases. Nonetheless, in this domain the dominant IMFs are either halfway between domains D1 and D2 or contain oscillations derived from the decomposition process. Figure 5.a shows the instantaneous frequency of the first and second IMFs for the case when $\omega_2 = 1.2\,\text{rad/s}$ and $E_a/E_{a,D} = 1.18$. The dominant IMF clearly has an oscillation around 250 s that is different from the original modes, causing an irregularity in the PTO damping

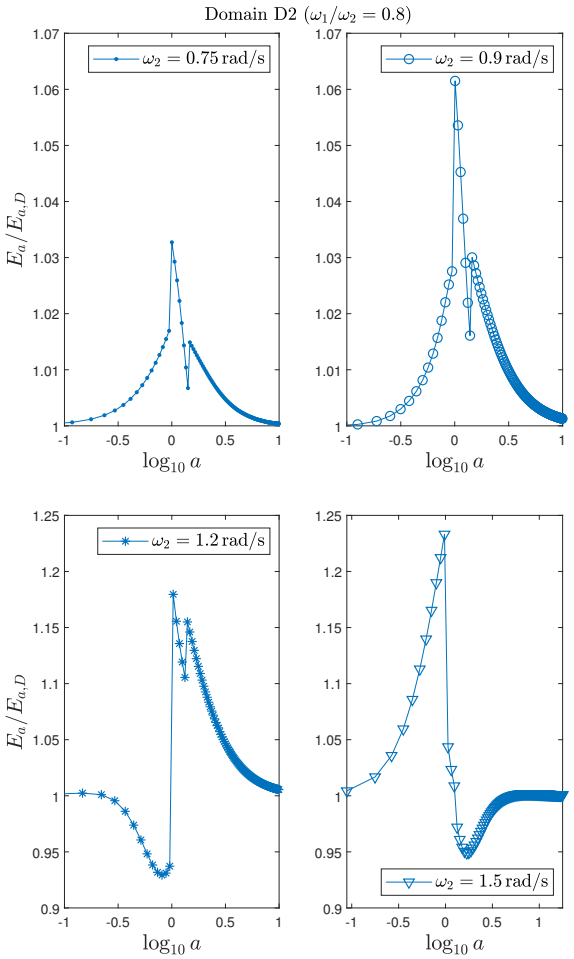

Fig. 2. Ratios between E_a and $E_{a,D}$ in domain D2.

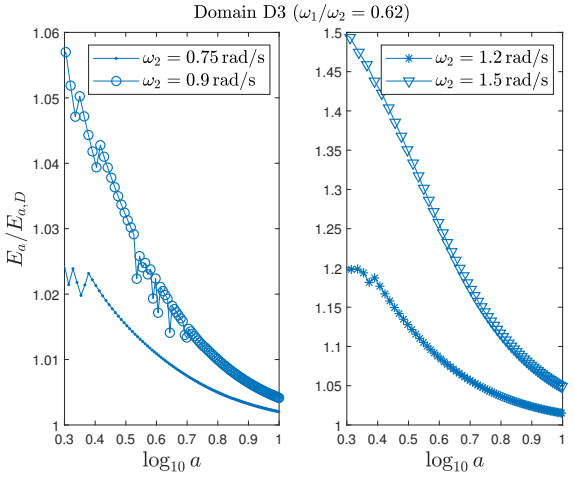

Fig. 3. Ratios between E_a and $E_{a,D}$ in domain D3.

profile (Fig. 5.b). Although the energy absorption is higher than the constant dominant frequency, such irregularity decreases the energy absorption in about 8% for the time interval 225 s to 255 s, when compared to the case the components are a single wave-form. Figure 6 shows the instantaneous frequency and the PTO damping for both the dominant IMF derived from EMD (IMF 1) and the analytic single wave-form for the case the components are together (i.e., single modulated components).

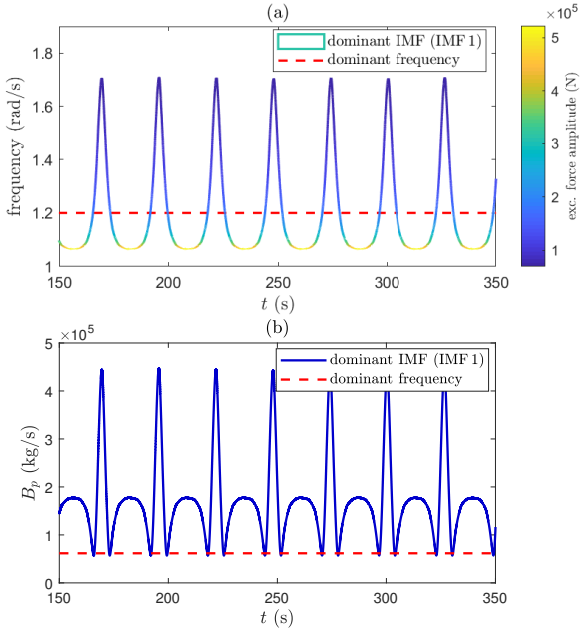

Fig. 4. Time-series for case $\omega_2 = 1.2$ rad/s, $E_a/E_{a,D} = 0.94$: (domain D2, $\omega_1/\omega_2 = 0.8$) (a) Hilbert spectrum for the first IMF, and constant dominant frequency; (b) PTO damping.

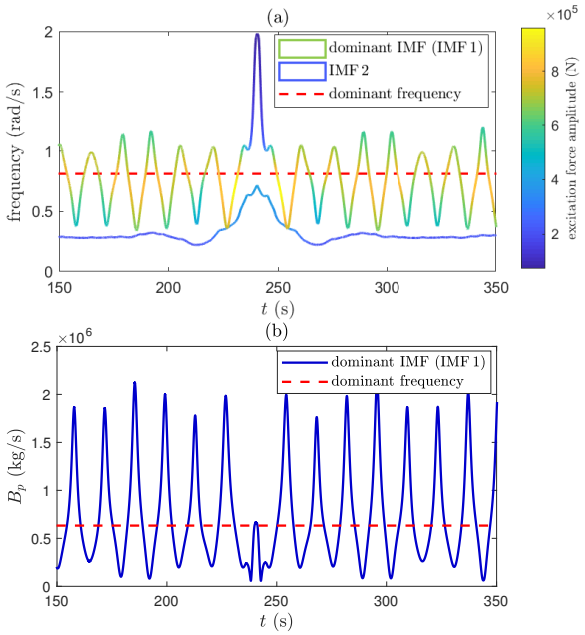

Fig. 5. Time-series for case $\omega_2 = 1.2$ rad/s, $E_a/E_{a,D} = 1.18$ (domain D3, $\omega_1/\omega_2 = 0.62$): (a) Hilbert spectrum for the first and second IMFs, and constant dominant frequency; (b) PTO damping.

B. Real ocean waves

Previous studies have shown that tuning the damping with frequency estimates from the HHT results in greater absorption of energy than tuning with estimates from EKF and FLL [2]. Here, the aim is to use the mode mixing conditions observed for the synthetic two-tone wave studies to further improve the energy absorbed by the HHT for real ocean waves that fulfill similar conditions. Therefore, we adopt two sea states (S1, S2) from the northeast coast of Brazil for the simulations. The wave elevation data consist of records of about 20 minutes (T 20 min) sampled at 1.28 Hz

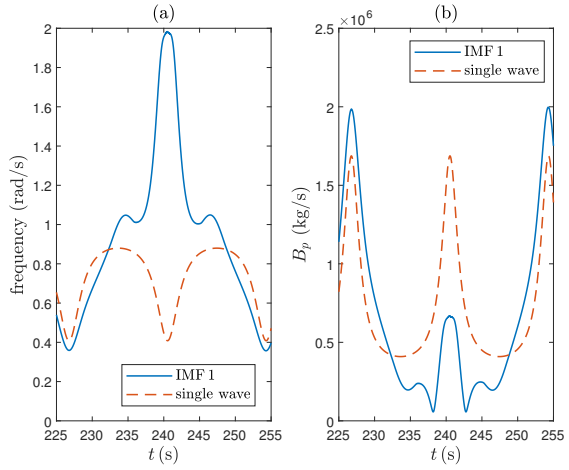

Fig. 6. (a) Instantaneous frequency, and (b) PTO damping for both the dominant IMF derived from EMD (solid line) and the analytic single wave-form (dashed line).

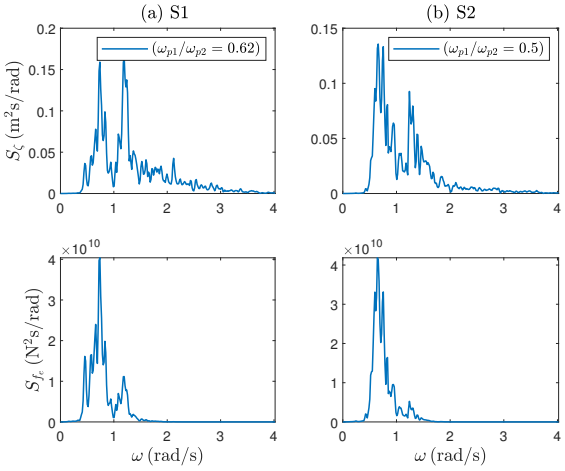

Fig. 7. Wave spectra from the northeast coast of Brazil (top) and excitation force spectra (bottom).

and registered by a wave buoy in the Port of Pecém area. Figure 7 shows two-peak wave spectra and the excitation force spectra for the cylinder. The frequency ratio for the peak frequencies (ω_{p1}/ω_{p2}) of the spectra are, 0.62 and 0.5, respectively, for sea states S1 and S2.

Figure 8 shows samples of time-series simulations for the excitation forces f_e, and the instantaneous frequencies for IMF 1 ($\hat{\omega}_d$, dominant IMF) and IMF 2. It can be noted that the IMFs consist of signals with similar frequency scales (mode mixing), and a similar behaviour between the real ocean waves and the synthetic two-tone waves (Fig. 5.a) is observed around 690 s (Fig. 8.a bottom) and 660 s (Fig. 8.b bottom).

The mode mixing could be attenuated by applying masking signals to the EMD, as done in, e.g., [8]. Conversely, here the mode mixing in domain D2 is beneficial to the energy absorption. However, the small oscillations on the PTO profile, caused either by the mode mixing in domain D3, or by the nature of the damping tuning equation (6), have a negative impact on the energy. Therefore, such oscillations are filtered out. Figure 9 shows the evolution of the PTO damping $B_p(t)$, and the body motion $x(t)$ for the cases when

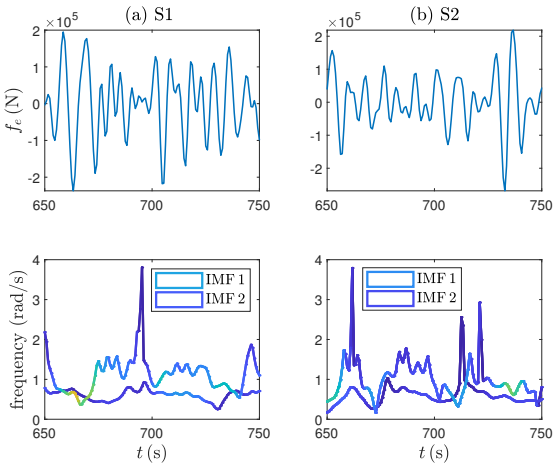

Fig. 8. Time-series of the excitation force, and instantaneous frequency of IMF 1 (dominant IMF) and IMF 2: (a) S1; (b) S2.

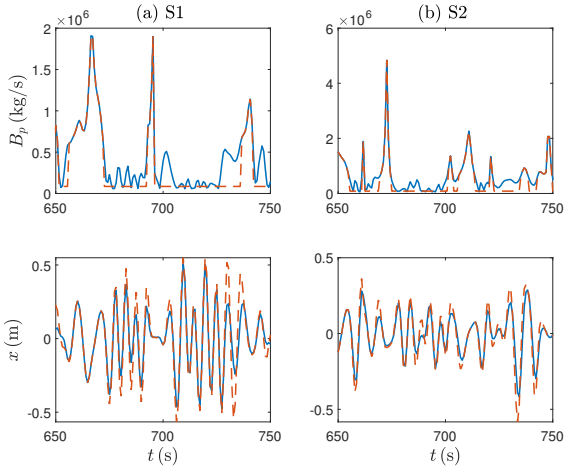

Fig. 9. Time-series of the PTO damping, and body motion: (a) S1; (b) S2. Solid lines: PC with HHT, dashed lines: PC with HHT and filtering of small damping oscillations.

the PTO damping is directly obtained from HHT and (6) (solid lines), and when the small PTO damping oscillations are filtered out (dashed lines). An energy improvement of about 2.6%, and 3.9%, is obtained for sea states S1, and S2, when the small damping oscillations are filtered out, which agrees with the two-tone signal studies in Section IV-A.

V. Conclusion

This study revealed how the EMD mode mixing problem affects the performance of WECs with a passive control strategy that tunes the PTO damping to frequency estimates from the HHT. The effect of mode mixing on the energy absorbed depends both on the type of IMF derived from the EMD procedure and the frequencies of the components (which is related to the frequency response of the floating body).

A comprehensive numerical study using synthetic two-tone waves showed that for mode mixing cases where components are decomposed as single waveforms (domain 2), the effect is beneficial to the absorption of energy if the constant dominant frequency is not the resonance frequency of the WEC. Additionally, the damping tuning law might result in small oscillations on the PTO profile that will negatively impact the energy absorption. For cases where the components are within two IMFs, or contain oscillations derived from the decomposition process (domain 3), the mode mixing effects might result in irregularities in the PTO damping profile that also decrease the absorption of energy. If the mode mixing causes a high peak in the instantaneous frequency of an IMF, the PTO damping will contain a small oscillation that is otherwise not present in the PTO damping profile.

The studies with synthetic two-tone waves were used to further improve the HHT absorbed energy for real ocean waves by filtering out the small oscillations on the PTO profile. An average energy improvement of 3.3% was obtained for two studied cases. Such oscillations in the damping are caused either by high-frequency oscillations derived from the EMD process or by the nature of the damping tuning equation (that is not optimized for the instantaneous frequency). Further studies are needed to determine the best damping tuning equation when the instantaneous frequency of waves is used as an input for the PTO tuning.

References

[1] P. B. Garcia-Rosa, G. Kulia, J. V. Ringwood, and M. Molinas, "Real-time passive control of wave energy converters using the Hilbert-Huang transform," in *IFAC-PapersOnLine*, vol. 50, no. 1 (Proc. of the 20th IFAC World Congress), Toulouse, France, 2017, pp. 14 705–14 710.

[2] P. B. Garcia-Rosa, J. V. Ringwood, O. B. Fosso, and M. Molinas, "The impact of time-frequency estimation methods on the performance of wave energy converters under passive and reactive control," *IEEE Trans. on Sustainable Energy*, (in press, DOI:10.1109/TSTE.2018.2870966), 2018.

[3] H. Yavuz, T. J. Stallard, A. P. McCabe, and G. A. Aggidis, "Time series analysis-based adaptive tuning techniques for a heaving wave energy converter in irregular seas," *Proc. of the Inst. of Mech. Engineers, Part A: Journal of Power and Energy*, vol. 221, no. 1, pp. 77–90, 2007.

[4] N. Tom and R. W. Yeung, "Nonlinear model predictive control applied to a generic ocean-wave energy extractor," in *Proc. of the 32nd International Conference on Ocean, Offshore and Arctic Engineering (OMAE 2013)*, Nantes, France, 2013.

[5] N. E. Huang, Z. Shen, S. R. Long, M. C. Wu, H. H. Shih, Q. Zheng, N.-C. Yen, C. C. Tung, and H. H. Liu, "The empirical mode decomposition and the Hilbert spectrum for nonlinear and non-stationary time series analysis," *Proc. Royal Society London*, vol. 454, pp. 903–995, 1998.

[6] N. E. Huang and Z. Wu, "A review on Hilbert-Huang transform: method and its applications to geophysical studies," *Review of Geophysics*, vol. 46, no. 2, 2007.

[7] R. Deering and J. F. Kaiser, "The use of a masking signal to improve empirical mode decomposition," in *Proc. of the IEEE Int. Conf. Acoustics, Speech, Signal Processing (ICASSP 05)*, Philadelphia, USA, 2005, pp. 485–488.

[8] O. B. Fosso and M. Molinas, "Method for mode mixing separation in empirical mode decomposition," *arXiv:1709.05547 [stat.ME]*, September 2017.

[9] Z. Wu and N. E. Huang, "Ensemble empirical mode decomposition: A noise-assisted data analysis method," *Advances in Adaptive Data Analysis*, vol. 1, no. 1, pp. 1–41, 2009.

[10] G. Rilling and P. Flandrin, "One or two frequencies? The empirical mode decomposition answers," *IEEE Trans. on Signal Processing*, vol. 56, no. 1, pp. 85–95, 2008.

[11] W. E. Cummins, "The impulse response function and ship motions," *Schiffstechnik*, vol. 47, no. 9, pp. 101–109, 1962.

[12] J. Falnes, *Ocean Waves and Oscillating Systems: Linear Interaction including Wave-Energy Extraction*. USA: Cambridge Univ. Press, 2002.

[13] B. Boashash, "Estimating and interpreting the instantaneous frequency of a signal - Part 1: Fundamentals." *Proc. of the IEEE*, vol. 80, no. 4, pp. 520–538, 1992.